International Journal on Advanced Science Engineering Information Technology

Vol.14 (2024) No. 1
ISSN: 2088-5334

Effectiveness of Vehicular Communication Using NP-CSMA with Bernoulli-Based Gaussian Interpolation Function

Mahmoud Zaki Iskandarani [a,*]

[a] *Faculty of Engineering, Al-Ahliyya Amman University, Amman, 19238, Jordan*
*Corresponding author: *m.iskandarani@ammanu.edu.jo*

Abstract— **The objective is to investigate the effectiveness of Gaussian arrival and its effect on vehicular communication compared to Bernoulli's arrival. MATLAB simulation covers three different levels of slot probability: low, medium, and high. The goal behind such simulation is to establish the importance of an adaptive function such as Gaussian interpolation resulting in smoother control of vehicular communication with better channel performance when compared to Bernoulli. This work shows that at low slot probability (Pslot), Gaussian arrival results in a much higher throughput (S) compared to Bernoulli, with a gradual reduction in throughput as Gaussian spread (γ) increases. The decrease in S as γ increases is due to the Gaussian interpolation, which performs control and results in higher channel stability. At mid probability, the simulation and analysis show a convergence between Gaussian results and Bernoulli, with differences in buffered frames (B_{total}) as a function of γ. At a high Pslot value, Bernoulli produces higher S than Gaussian, with the closest Gaussian values at γ=2. However, the number of buffered frames using Bernoulli arrival is much higher than Gaussian. The exceedingly high B_{total} can result in more collisions, which Gaussian arrival controls very well with a small sacrifice in throughput. The shape function for Bernoulli is shown to be different from Gaussian, except for specific values of γ, where there is a match. The obtained results show the adaptability and smoothness in which Gaussian arrival can optimize channel communication using Non-Persistent CSMA, which enables intelligent vehicular communication.**

Keywords—**NP-CSMA; connected vehicles; network connectivity; Bernoulli; data traffic; throughput; Gaussian interpolation; slot probability.**

Manuscript received 24 Feb. 2023; revised 31 Oct. 2023; accepted 3 Jan. 2024. Date of publication 29 Feb. 2024.

I. INTRODUCTION

For many years, the automotive industry has been designing in-vehicle systems to detect possible accident situations in advance and warn the driver or navigate the vehicle. Such systems use an active safety approach. Active safety systems can avoid many accidents that could otherwise occur today due to drivers' decision-making. For such active and preventative systems to operate successfully, each vehicle needs to know the locations and motions of its neighboring cars [1]–[6].

To achieve this knowledge, each vehicle sends a basic safety message (BSM) many time per minute to enable other vehicles and to determine its position and motion parameters [7]–[11]. This is accomplished using media access control protocols (MAC) within the vehicular ad hoc network structure (VANET) for temporary networks formed by vehicles within a certain range [12]–[14] The process is based on random access concept, with avoidance of coordination with base stations or a roadside infrastructure, using a decentralized approach. Traffic volumes and vehicles' dynamic nature and mobility could present challenging issues regarding successfully delivering BSMs within acceptable time limits. In addition, hidden terminals may manifest. Retransmitting a message more than once raises the probability of reception and the possibility of collision, as generated data traffic increases significantly [15], [16].

One of the most extensively used Media Access Control (MAC) protocols, Carrier Sense Several Access (CSMA), enables multiple users to share a single transmission channel, such as Ethernet and 802.11 wireless LAN. Carrier Sense Multiple Access (CSMA) is a much research and applied Media Access Control (MAC) protocols, as it allows multiple users to share a common communication medium [17], [18], [19], [20].

Connectivity times are critical parameters using CSMA in networks using carrier sensing multiple access with collision avoidance (CSMA/CA) approach, which affects the network bandwidth and the node throughput. Several techniques use idle/busy time to estimate network performance. Exploring the idle time duration is important in radio networks where networks reuse resources not only in the spatial and temporal domains [21]–[26].

Using the Non-Persistent Carrier-Sense Multiple Access (NP-CSMA) protocol, each node acts after sensing the status of the communication channel. If the channel idles, the packet is transmitted immediately; otherwise, the packet is kept for a random amount of time before sensing the channel again. Collisions could occur when two or more packets are transmitted within a very short time of each other. The maximum throughput for NP-CSMA can be derived using the semi-Markovian model. Collisions will occur in a shared communication environment, and a contention resolution algorithm is a core in any MAC protocol to resolve contention between communicating nodes [27]–[30].

Most MAC protocols implement the exponential Backoff algorithm in many collision resolution schemes. However, Exponential Backoff for MAC protocols are unstable for an infinite number of nodes about the arrival rate. When the arrival rate of the system is small, the Exponential Backoff can still be stable despite the large number of nodes. Thus, arrival rate is a primary factor in optimizing network performance, correlating to throughput [31]–[35].

1P-CSMA consumes excessive time due to continuous listening channels, which is unsuitable for vehicular communication. However, NP-CSMA takes the NP-CSMA (non-persistent CSMA) and 1P-CSMA characteristics by adjusting the probability and collision rate to achieve higher throughput under heavy load.

NP-CSMA protocol adds functionality to the random protocols and senses the medium to determine whether any other node (user) is transmitting. Despite all these collision avoidance approaches, networks are still affected by packet collisions, which affect throughput and reduce system performance [36]–[40].

This work investigates through simulation the effectiveness of using the Gaussian Interpolation function to modulate arrival times on the effectiveness and stability of NP-CSMA, which uses Bernoulli arrival time for vehicular Medium Access Control (MAC). The work simulates both approaches and compares Bernoulli-based NP-CSMA and Gaussian-based NP-CSMA. The rest of this paper is divided as follows: Material and Method, Results and Discussion, Conclusions, References.

II. Materials and Method

The approach in this work operates on analyzing the simulated results obtained for various Gaussian Spread values (using Gaussian arrival) as a function of slot probability and for a variable slot probability (using Bernoulli arrival). The following parameters were used in the simulation:

- V_{node}: 15
- γ: {2, 4, 8, 16, 32}
- Slot Probability: {0.005, 0.05, 0.5}
- Total Slot Number: 7500
- Waiting Time: 20 Slots
- Backoff Time: 19
- Fame Length: 5

Assumptions:

- The number of users (nodes) is finite, and two arrival processes are used: Bernoulli and Gaussian.
- Carrier sensing takes place instantly
- The communication channel is noise-
- Transmission failure is related to collisions, slot probability, and Gaussian interpolation coefficient.
- Transmitted data is of equal size for all vehicular nodes.

In the MATLAB simulation, an arrival probability (P_{arrive}) value is randomly generated with two cases applied:

1) Bernoulli case: P_{arrive} is randomly generated and compared to slot probability (P_{slot}) as shown in equation (1).

$$Bernoulli_{arrival} = |P_{arrive} - P_{slot}| \tag{1}$$

2) Gaussian Interpolation case: P_{arrive} is substituted into equation (2) and then compared to P_{slot}.

$$Gaussian_{arrival} = exp\left(\frac{-((P_{arrive}-P_{slot})^2)}{2\gamma}\right) \tag{2}$$

From equations (1) and (2), equation (3) is obtained.

$$Gaussian_{arrival} = exp\left(\frac{-((Bernoulli_{arrival})^2)}{2\gamma}\right) \tag{3}$$

The expression in equation (3) represents an adaptive approach to vehicular connectivity, which should enable more efficient and effective communication. In addition, equation (3) allows for intelligent, smooth, and adaptive multiple access communication, as it has both exponential functionality and the spread parameter, which optimizes the communication channel performance. Table I shows the used acronyms and their definition.

TABLE I
NOMENCLATURE

Symbols/Acronyms	Meaning
V_{node}	Nodes Number: Number of vehicles that generate packets.
P_{slot}	Slot probability is the probability that a specific node or station has data ready to transmit at a particular time slot.
S	Throughput of the NP-CSMA protocol
G	Normalized available traffic, with retransmissions included.
B_{total}	Total buffered number of frames.
γ	Gaussian spread
N1	Number of response points in a G-S curve before the inflection point.
N2	Number of response points in a G-S curve after inflection point.
F_{gen}	Generated frames
S_{avg}	Average throughput as a function of slot probability
G_{avg}	Average data traffic as a function of slot probability

III. Results and Discussion

Figures 1 to 6 show the relationship between G and S, using both Bernoulli and Gaussian arrivals, for P_{slot}=0.005, and γ= {2, 4, 8, 16, 32}. From the Figures, it is evident that there is a marked difference in the shape function using Bernoulli compared to the response using Gaussian. It is also clear from Table II that G and G_{avg} values using Gaussian arrival are much higher at P_{slot}=0.005 compared to Bernoulli values. It is also clear that as the Gaussian spread increases, G_{avg} decreases, indicating smoother and better data traffic control and interpolation. Table III shows the effect of Gaussian spread on S. From the presented data, using Gaussian arrival time will enable higher throughput than Bernoulli's arrival time. However, in correlation to G_{avg} reduction as γ increases, S_{avg} will suffer a reduction in value, but it indicates more stable connectivity. Table IV further supports Tables II and III, as it shows several buffered frames. As presented in the Table, B_{total} for using Gaussian arrival is much higher at P_{slot}=0.005 compared to Bernoulli, with the average value decreases as γ increases. This further supports that the communication channels are more stable with less collision probability.

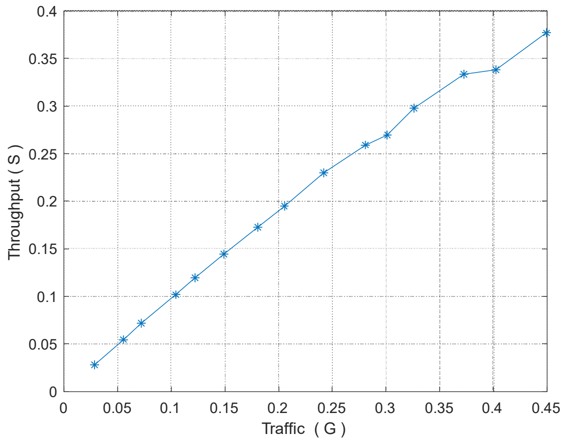

Fig. 1 Relationship between throughput and traffic for P_{slot} =0.005 using Bernoulli arrival.

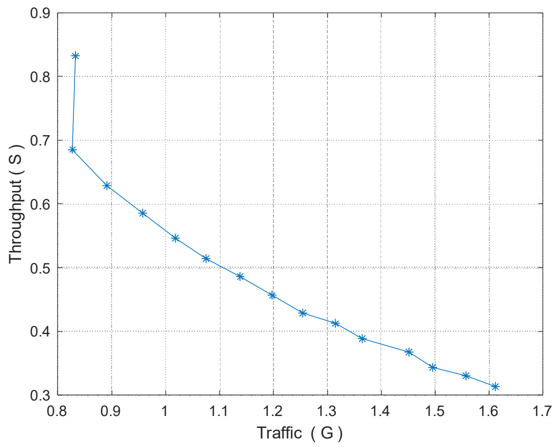

Fig. 2 Relationship between throughput and data traffic for P_{slot} =0.005 using Gaussian arrival with γ=2.

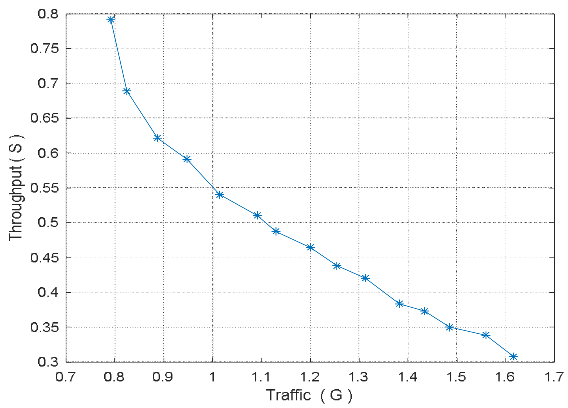

Fig. 3 Relationship between throughput and data traffic for P_{slot} =0.005 using Gaussian arrival with γ=4.

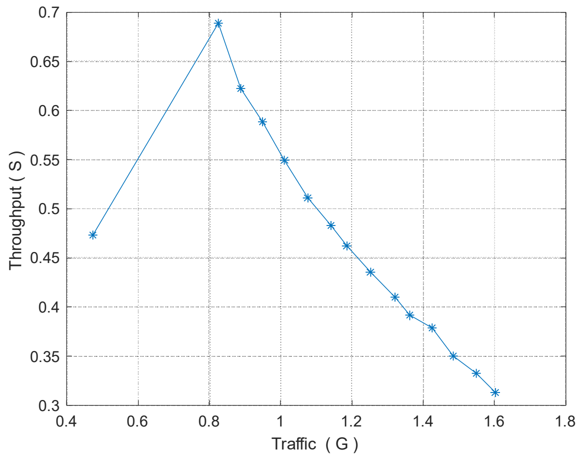

Fig. 4 Relationship between throughput and data traffic for P_{slot} =0.005 using Gaussian arrival with γ=8.

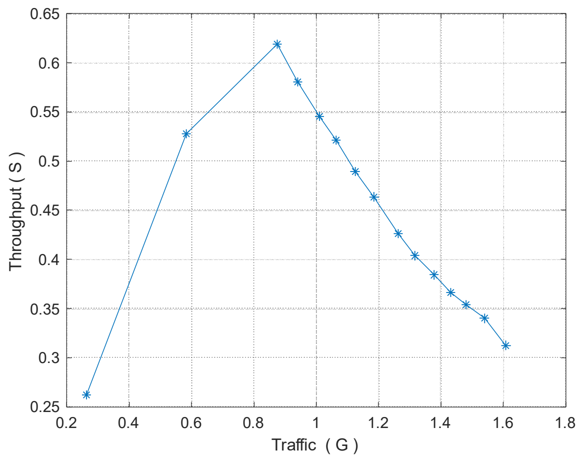

Fig. 5 Relationship between throughput and data traffic for P_{slot} =0.005 using Gaussian arrival with γ=16.

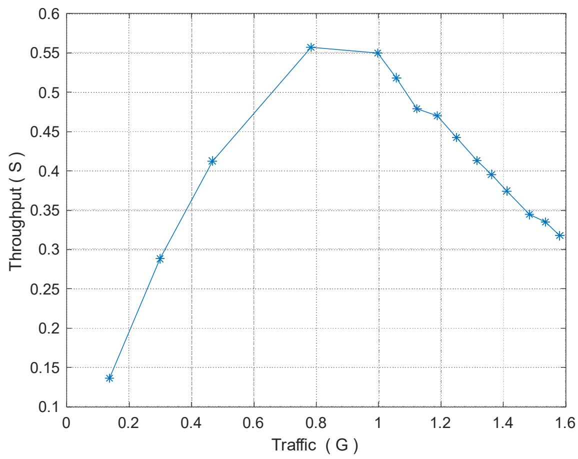

Fig. 6 Relationship between throughput and data traffic for P_{slot} =0.005 using Gaussian arrival with γ=32.

TABLE II

RELATIONSHIP BETWEEN SLOT PROBABILITY AND BUFFERED FRAMES

P_{slot}=0.005						
Data Traffic						
V_{node}	γ=2	γ=4	γ=8	γ=16	γ=32	Bernoulli
1	0.833	0.792	0.473	0.262	0.137	0.028
2	0.827	0.824	0.825	0.583	0.299	0.056
3	0.890	0.888	0.888	0.875	0.466	0.072
4	0.957	0.947	0.949	0.940	0.782	0.104
5	1.018	1.015	1.011	1.010	0.996	0.122

P_{slot}=0.005						
Data Traffic						
V_{node}	γ=2	γ=4	γ=8	γ=16	γ=32	Bernoulli
6	1.075	1.092	1.076	1.064	1.057	0.149
7	1.138	1.130	1.141	1.124	1.123	0.180
8	1.198	1.201	1.185	1.186	1.188	0.205
9	1.254	1.254	1.252	1.263	1.249	0.242
10	1.314	1.313	1.321	1.317	1.315	0.281
11	1.364	1.382	1.362	1.378	1.362	0.301
12	1.451	1.434	1.425	1.432	1.411	0.326
13	1.495	1.484	1.484	1.481	1.484	0.373
14	1.557	1.559	1.549	1.539	1.536	0.403
15	1.611	1.616	1.602	1.608	1.581	0.450
Average	1.199	1.196	1.170	1.137	1.066	0.220

TABLE III

RELATIONSHIP BETWEEN SLOT PROBABILITY AND BUFFERED FRAMES

Pslot=0.005						
Throughput						
V_{node}	γ=2	γ=4	γ=8	γ=16	γ=32	Bernoulli
1	0.832	0.7913	0.473	0.262	0.136	0.028
2	0.685	0.6889	0.689	0.528	0.288	0.055
3	0.628	0.6213	0.622	0.619	0.413	0.072
4	0.585	0.5911	0.589	0.581	0.557	0.102
5	0.546	0.54	0.550	0.545	0.550	0.119
6	0.514	0.5102	0.511	0.521	0.518	0.145
7	0.486	0.4873	0.483	0.490	0.479	0.172
8	0.456	0.4642	0.462	0.464	0.470	0.195
9	0.429	0.438	0.436	0.426	0.442	0.230
10	0.412	0.4204	0.410	0.404	0.413	0.259
11	0.389	0.3836	0.392	0.384	0.396	0.269
12	0.368	0.3731	0.379	0.366	0.374	0.298
13	0.343	0.35	0.350	0.354	0.344	0.334
14	0.330	0.3382	0.333	0.340	0.335	0.338
15	0.314	0.3078	0.313	0.312	0.318	0.377
Average	0.488	0.487	0.466	0.440	0.402	0.200

TABLE IV

RELATIONSHIP BETWEEN SLOT PROBABILITY AND BUFFERED FRAMES

P_{slot}=0.005						
Buffered Frames						
V_{node}	γ=2	γ=4	γ=8	γ=16	γ=32	Bernoulli
1	1813	1109	690	361	180	0
2	1820	1198	705	392	169	0
3	1875	1115	675	376	173	0
4	1714	1221	708	363	198	0
5	1734	1189	678	402	180	0
6	1804	1220	693	385	171	1
7	1786	1149	724	366	193	0
8	1783	1142	694	384	197	0
9	1771	1184	683	356	207	1
10	1849	1161	703	406	202	0
11	1881	1189	711	363	193	0
12	1832	1163	689	347	168	2
13	1795	1128	672	336	165	0
14	1853	1147	666	349	166	0
15	1778	1191	645	369	180	1
Average	27088	17506	10336	5555	2742	5

Figures 7 to 12 show the relationship between G and S, using both Bernoulli arrival and Gaussian arrival, for P_{slot}=0.05, and γ= {2, 4, 8, 16, 32}. From the Figures, it is evident that there is a marked difference in the shape function using Bernoulli compared to the response using Gaussian. In addition, the Bernoulli response curve at P_{slot}=0.05 shows similar shape features to Gaussian response curve at P_{slot}=0.005 and γ=16. It is also clear from Tables V that G and G_{avg} values using Gaussian arrival are converging to the Bernoulli ones at P_{slot}=0.05, except at γ=32, where G_{avg} using Gaussian arrival is less than Bernoulli. This is due to the increase in slot probability, which is more controllable and provides smoother transition of data traffic and throughout using Gaussian arrival compared to the binary form of Bernoulli.

In correlation with these results, Table VI shows the S and S_{avg} results, which indicates that the throughput using Gaussian arrival is higher compared to Bernoulli, except at γ=32, where Bernoulli arrival results in higher S_{avg} values. Table VII shows the effect of using Gaussian arrival compared to Bernoulli on buffered frames. From the Table, the influence and power of Gaussian is evident, as the number of buffered frames and their total B_{total} is less at γ=32 compared to Bernoulli, with a noticeable increase in the buffered frames using Bernoulli. Thus, using Gaussian arrival provides the required adaptability and control to enable more efficient communication and connectivity using the spread parameter to achieve balanced and effective throughput with minimum number of collisions.

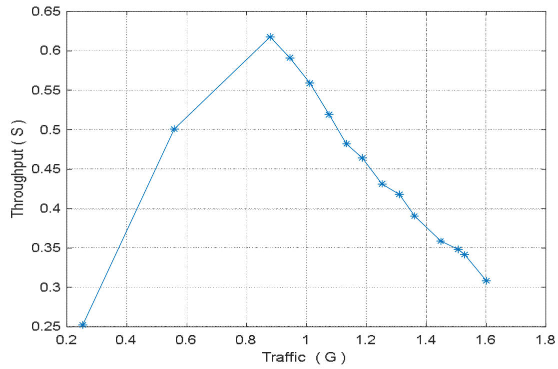

Fig. 7 Relationship between throughput and data traffic for P_{slot} =0.05 using Bernoulli arrival.

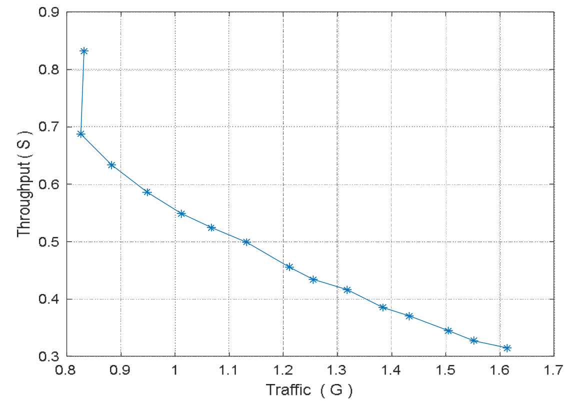

Fig. 8 Relationship between throughput and data traffic for P_{slot} =0.05 using Gaussian arrival with γ=2.

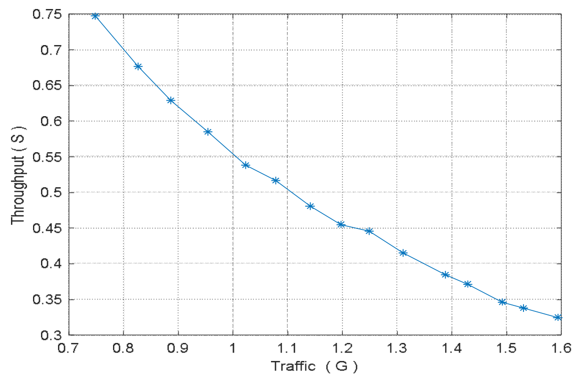

Fig. 9 Relationship between throughput and data traffic for P_{slot} =0.05 using Gaussian arrival with γ=4.

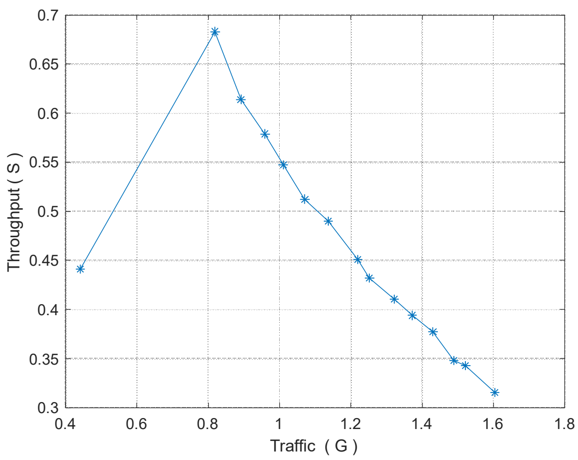

Fig. 10 Relationship between throughput and data traffic for P_{slot} =0.05 using Gaussian arrival with γ=8.

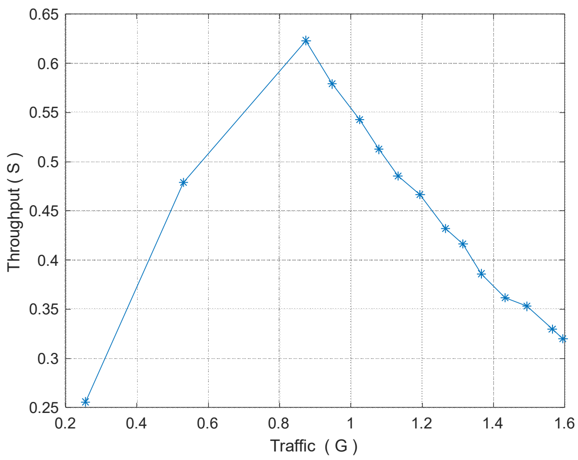

Fig. 11 Relationship between throughput and data traffic for P_{slot} =0.05 using Gaussian arrival with γ=16.

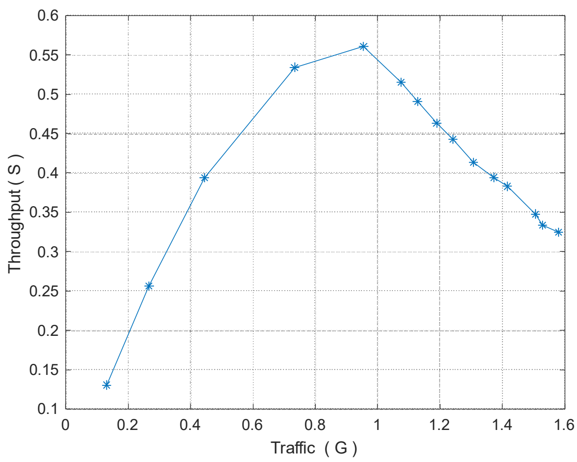

Fig. 12 Relationship between throughput and data traffic for P_{slot} =0.05 using Gaussian arrival with γ=32.

TABLE V

RELATIONSHIP BETWEEN SLOT PROBABILITY AND BUFFERED FRAMES

P_{slot}=0.05						
Data Traffic						
V_{node}	**γ=2**	**γ=4**	**γ=8**	**γ=16**	**γ=32**	**Bernoulli**
1	0.832	0.748	0.442	0.256	0.130	0.253
2	0.826	0.827	0.819	0.530	0.267	0.559
3	0.883	0.886	0.892	0.874	0.444	0.879
4	0.948	0.954	0.960	0.947	0.733	0.945

P_{slot}=0.05						
Data Traffic						
V_{node}	**γ=2**	**γ=4**	**γ=8**	**γ=16**	**γ=32**	**Bernoulli**
5	1.012	1.023	1.010	1.024	0.955	1.010
6	1.067	1.078	1.071	1.079	1.075	1.075
7	1.132	1.141	1.137	1.132	1.128	1.134
8	1.212	1.198	1.219	1.194	1.189	1.186
9	1.255	1.249	1.252	1.265	1.242	1.252
10	1.318	1.311	1.322	1.315	1.308	1.310
11	1.384	1.388	1.372	1.366	1.373	1.360
12	1.433	1.429	1.430	1.432	1.416	1.448
13	1.504	1.492	1.489	1.493	1.507	1.506
14	1.552	1.531	1.522	1.565	1.529	1.527
15	1.613	1.593	1.604	1.595	1.580	1.601
Average	1.198	1.190	1.169	1.138	1.058	1.136

TABLE VI

RELATIONSHIP BETWEEN SLOT PROBABILITY AND BUFFERED FRAMES

P_{slot}=0.05						
Throughput						
V_{node}	**γ=2**	**γ=4**	**γ=8**	**γ=16**	**γ=32**	**Bernoulli**
1	0.832	0.747	0.441	0.256	0.130	0.252
2	0.688	0.677	0.683	0.479	0.256	0.501
3	0.634	0.629	0.614	0.623	0.394	0.618
4	0.586	0.585	0.579	0.579	0.534	0.591
5	0.549	0.538	0.547	0.543	0.561	0.559
6	0.524	0.517	0.512	0.512	0.515	0.519
7	0.499	0.481	0.490	0.485	0.491	0.482
8	0.456	0.455	0.451	0.466	0.463	0.464
9	0.434	0.446	0.432	0.432	0.443	0.431
10	0.416	0.415	0.410	0.416	0.414	0.418
11	0.385	0.385	0.394	0.386	0.394	0.391
12	0.370	0.372	0.378	0.362	0.383	0.358
13	0.345	0.346	0.348	0.353	0.348	0.348
14	0.328	0.338	0.343	0.330	0.334	0.341
15	0.314	0.325	0.316	0.320	0.325	0.308
Average	0.491	0.484	0.463	0.436	0.399	0.439

TABLE VII

RELATIONSHIP BETWEEN SLOT PROBABILITY AND BUFFERED FRAMES

P_{slot}=0.05						
Buffered Frames						
V_{node}	**γ=2**	**γ=4**	**γ=8**	**γ=16**	**γ=32**	**Bernoulli**
1	1640	1059	687	325	171	361
2	1704	1116	620	357	162	319
3	1718	1088	604	382	153	335
4	1713	1111	655	339	170	340
5	1746	1057	630	348	184	314
6	1693	1027	666	323	130	348
7	1695	1058	626	321	150	349
8	1675	1037	595	374	141	343
9	1717	1054	626	338	175	336
10	1688	1072	621	353	182	345
11	1665	1112	644	359	174	336
12	1608	1070	602	307	188	349
13	1698	1089	642	281	159	388
14	1661	1051	627	324	149	350
15	1743	1051	655	321	175	372
Average	25364	16052	9500	5052	2463	5185

Figures 13 to 18 show the relationship between G and S, using both Bernoulli arrival and Gaussian arrival, for P_{slot}=0.5, and γ= {2, 4, 8, 16, 32}. From the Figures, it is evident that there is a marked difference in the shape function using Bernoulli compared to the response using Gaussian. In addition, the Bernoulli response curve at P_{slot}=0.5 shows similar shape features to Gaussian response curve at

P_{slot}=0.005 and γ=2, and P_{slot}=0.05 and γ=2. It is also clear from Tables VIII that G and $G_{avg\ values}$ using Gaussian arrival are converging to the Bernoulli ones at P_{slot}=0.5, except at γ=32, where G_{avg} using Gaussian arrival is less than Bernoulli. The is due to the increase in slot probability, with Gaussian arrival provides smoother transition of data traffic with better control using γ compared to the binary Bernoulli arrival.

In correlation with these results, Table IX shows the S and S_{avg} results, which indicates that the throughput using Gaussian arrival is lower compared to Bernoulli (closest value is at γ=2), especially at γ=32, where Bernoulli arrival results in a much higher S_{avg} values. Table X shows the effect of using Gaussian arrival compared to Bernoulli on frame buffering. From the Table, the influence and power of Gaussian is evident, as the number of buffered frames and their total B_{total} is much less than Bernoulli, particularly at γ=32. This is an indication of the higher efficiency and effectiveness using Gaussian arrival compared to Bernoulli. The other fact is that Gaussian arrival can be tuned and optimized, which provides the much-needed flexibility to enable adaptive networking and communication for vehicles and mobile nodes.

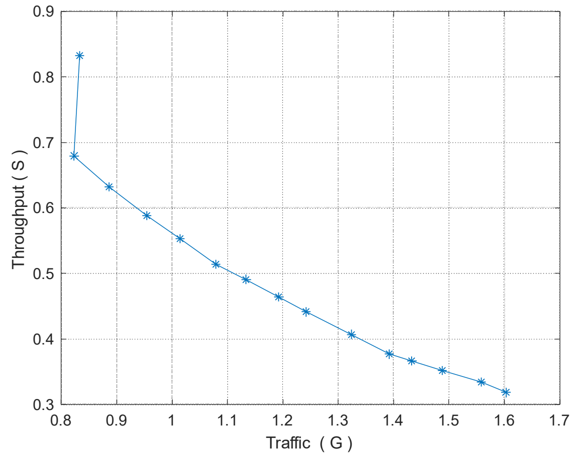

Fig. 13 Relationship between throughput and data traffic for P_{slot} =0.5 using Bernoulli arrival.

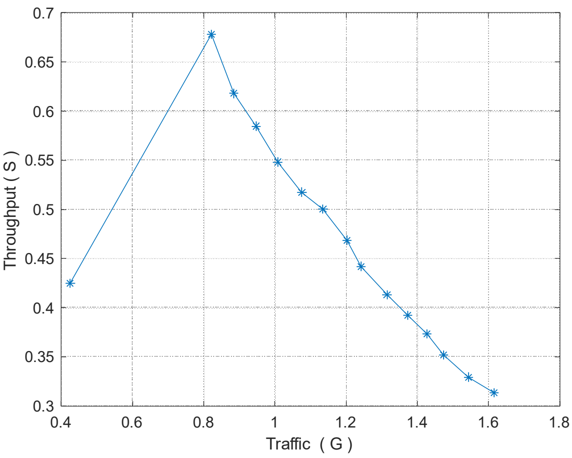

Fig. 14 Relationship between throughput and data traffic for P_{slot} =0.5 using Gaussian arrival with γ=2.

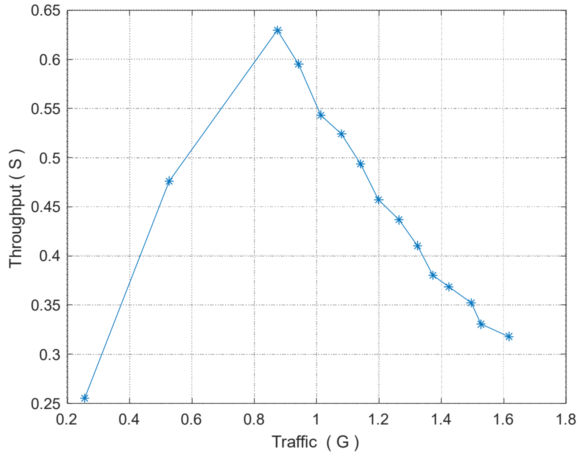

Fig. 15 Relationship between throughput and data traffic for P_{slot} =0.5 using Gaussian arrival with γ=4.

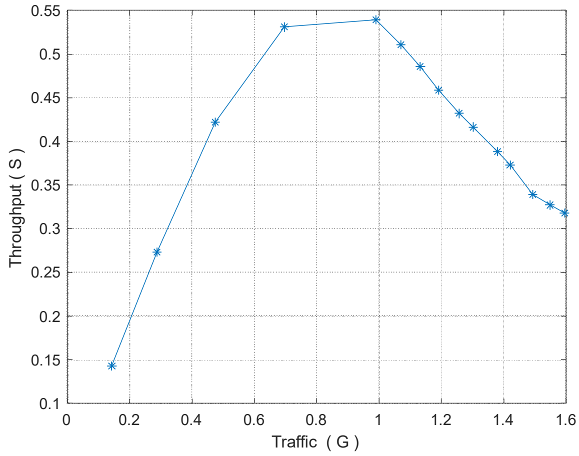

Fig. 16 Relationship between throughput and data traffic for P_{slot} =0.5 using Gaussian arrival with γ=8.

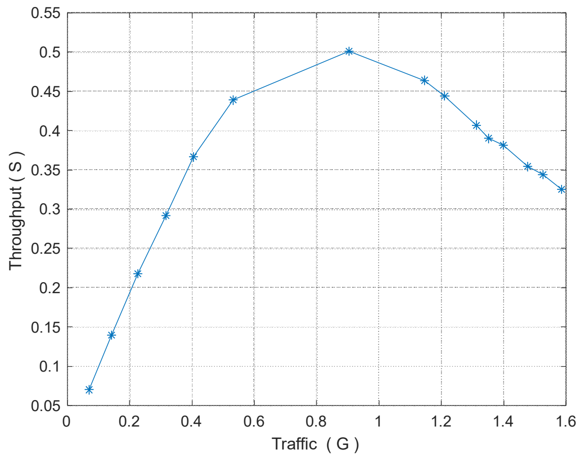

Fig. 17 Relationship between throughput and data traffic for P_{slot} =0.5 using Gaussian arrival with γ=16.

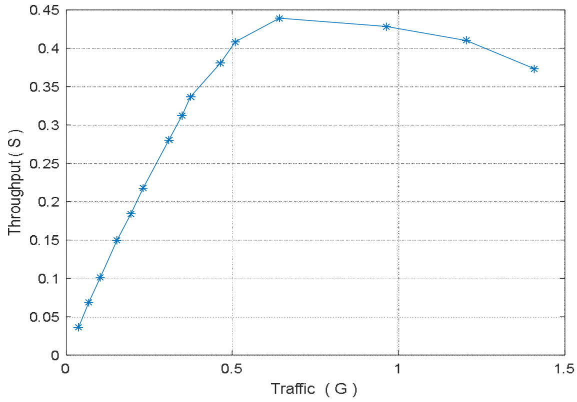

Fig. 18 Relationship between throughput and data traffic for P_{slot} =0.5 using Gaussian arrival with γ=32.

TABLE VIII
RELATIONSHIP BETWEEN SLOT PROBABILITY AND BUFFERED FR,AMES

P_{slot}=0.5						
Data Traffic						
V_{node}	γ=2	γ=4	γ=8	γ=16	γ=32	Bernoulli
1	0.425	0.255	0.143	0.070	0.037	0.833
2	0.821	0.527	0.288	0.142	0.069	0.823
3	0.884	0.875	0.474	0.226	0.102	0.886
4	0.948	0.942	0.696	0.316	0.153	0.954
5	1.008	1.014	0.990	0.404	0.196	1.014
6	1.076	1.080	1.070	0.532	0.232	1.079
7	1.135	1.141	1.132	0.904	0.310	1.134
8	1.202	1.199	1.191	1.146	0.349	1.193
9	1.242	1.264	1.256	1.211	0.375	1.242
10	1.315	1.324	1.302	1.312	0.464	1.324
11	1.373	1.372	1.380	1.352	0.510	1.392
12	1.427	1.423	1.420	1.399	0.642	1.433
13	1.474	1.495	1.493	1.476	0.964	1.488
14	1.544	1.526	1.548	1.525	1.205	1.558
15	1.615	1.618	1.595	1.585	1.409	1.603
Average	1.166	1.137	1.065	0.907	0.468	1.197

TABLE IX
RELATIONSHIP BETWEEN SLOT PROBABILITY AND BUFFERED FRAMES

P_{slot}=0.5						
Throughput						
V_{node}	γ=2	γ=4	γ=8	γ=16	γ=32	Bernoulli
1	0.425	0.2551	0.143	0.070	0.036	0.833
2	0.678	0.4762	0.273	0.140	0.069	0.680
3	0.618	0.6298	0.422	0.218	0.101	0.632
4	0.585	0.5953	0.531	0.292	0.150	0.588
5	0.548	0.5433	0.539	0.366	0.184	0.553
6	0.518	0.5242	0.511	0.439	0.218	0.514
7	0.500	0.4936	0.486	0.501	0.280	0.491
8	0.469	0.4569	0.458	0.464	0.312	0.464
9	0.442	0.4367	0.432	0.444	0.337	0.441
10	0.413	0.4104	0.416	0.407	0.381	0.407
11	0.392	0.3802	0.388	0.390	0.408	0.377
12	0.374	0.3687	0.373	0.381	0.439	0.367
13	0.352	0.3522	0.339	0.354	0.428	0.352
14	0.329	0.3304	0.327	0.344	0.410	0.334
15	0.314	0.318	0.318	0.325	0.373	0.318
Average	0.464	0.438	0.397	0.342	0.275	0.490

TABLE X
RELATIONSHIP BETWEEN SLOT PROBABILITY AND BUFFERED FRAMES

P_{slot}=0.5						
Buffered Frames						
V_{node}	γ=2	γ=4	γ=8	γ=16	γ=32	Bernoulli
1	600	355	190	93	8	3713
2	590	315	171	81	15	3671
3	545	323	191	86	9	3704
4	574	333	163	67	27	3712
5	566	332	165	82	7	3650
6	579	351	217	67	11	3701
7	608	319	158	75	36	3657
8	640	330	159	68	6	3707
9	618	312	168	102	18	3750
10	624	307	188	64	5	3757
11	581	338	177	51	22	3772
12	607	342	166	80	21	3695
13	622	337	171	86	27	3730
14	604	367	192	80	17	3669
15	564	360	147	88	23	3795
Average	8922	5021	2623	1170	252	55683

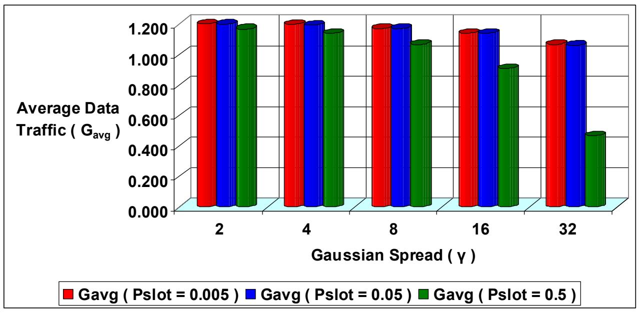

Fig. 19 Comparison between data traffic for different γ values as a function of P_{slot} using Gaussian arrival.

Figure 19 shows the effect of γ on G_{avg} using Gaussian arrival as a function of different P_{slot}, while Figure 20 shows a comparison of G_{avg} as a function of P_{slot}. From the Figures and equations (4) and (5), it is evident the different characteristics and functional behavior for each arrival technique, which affects the shape function response, and the resulted data traffic. This can be optimized using Gaussian arrival spread:

$$G_{avg(P_{slot},Gaussian)} = \alpha exp(-\beta\gamma) \quad (4)$$

where
$\alpha \geq 1.2, \beta \geq 0.004\ for\ P_{slot} = 0.005\ and\ 0.05$
$\alpha \geq 1.3, \beta \geq 0.03\ for\ P_{slot} = 0.5.$

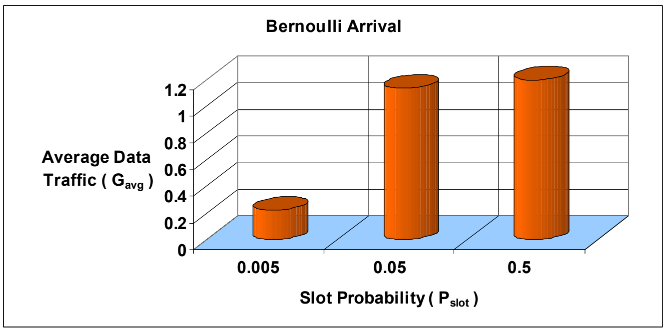

Fig. 20 Comparison between data traffic for different P_{slot} values using Bernoulli arrival.

$$G_{avg(P_{slot},Bernoulli)} = \mu Log_e(P_{slot}) + \rho \quad (5)$$

where $\mu \geq 0.2, \rho \leq 1.5$.

Figure 21 shows the effect of γ on S_{avg} using Gaussian arrival as a function of different P_{slot}, while Figure 22 shows a comparison of G_{avg} as a function of P_{slot}. From the Figures and equations (6) and (7), it is also evident the different characteristics and functional behavior for each arrival technique, which affects the shape function response, and the resulted throughput. This can be optimized using Gaussian arrival spread.

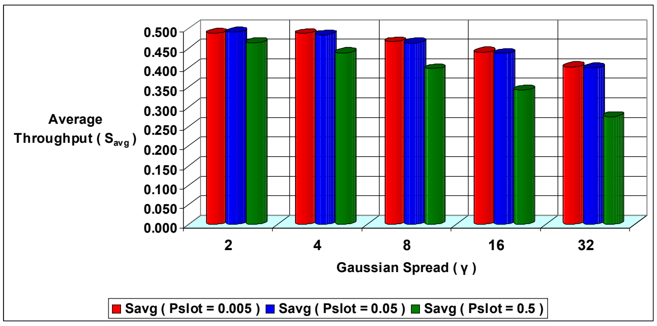

Fig. 21 Comparison between throughput for different P_{slot} values using Gaussian arrival.

$$S_{avg(P_{slot})} = \psi exp(-\theta\gamma) \quad (6)$$

where
$\psi \leq 0.5, \theta \leq 0.007\ for\ P_{slot} = 0.005\ and\ 0.05.$
$\psi \leq 0.5, \theta \leq 0.02\ for\ P_{slot} = 0.5$

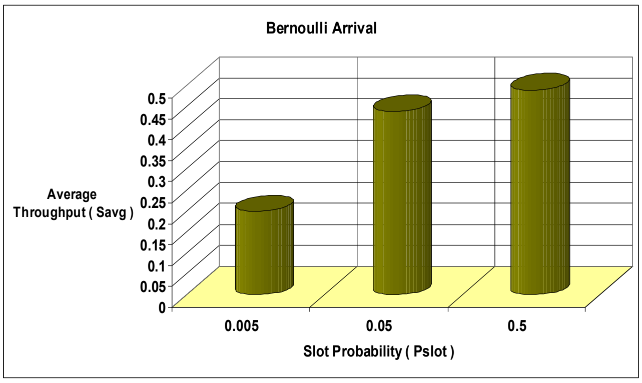

Fig. 22 Comparison between throuhput for different P_{slot} values using Bernoulli arrival.

$$S_{avg(P_{slot},Bernoulli)} = \mu Log_e(P_{slot}) + \rho \quad (7)$$

where $\mu \geq 0.06, \rho \geq 0.55$.

Figure 23 shows the effect of γ on B_{total} using Gaussian arrival as a function of different P_{slot}, while Figure 24 shows a comparison of B_{total} as a function of P_{slot}. From the Figures and equations (8) and (9), it is also evident the different characteristics and functional behavior for each arrival technique, which affects the shape function response, and the resulted throughput. Equation (8) reflects the binary nature of Bernoulli arrival, which does not lend itself to smooth optimization. In contrast to possible optimization using Gaussian arrival spread.

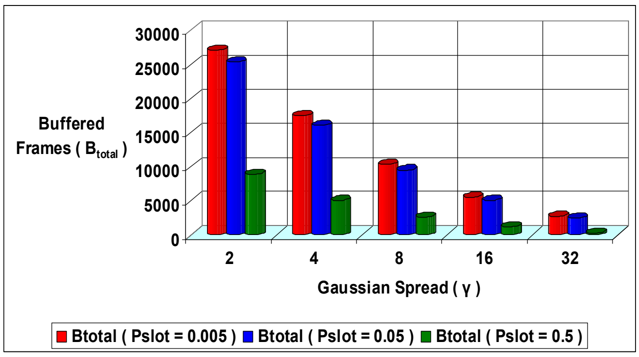

Fig. 23 Comparison between buffered frames for different P_{slot} values using Gaussian arrival.

$$B_{total(P_{slot})} = \phi\gamma^{-\omega} \quad (8)$$

where
$\phi \geq 52600, \omega \geq 0.83\ for\ P_{slot} = 0.005$
$\phi \geq 49515, \omega \geq 0.83\ for\ P_{slot} = 0.05$
$\phi \leq 26740, \omega \geq 1.2\ for\ P_{slot} = 0.5$

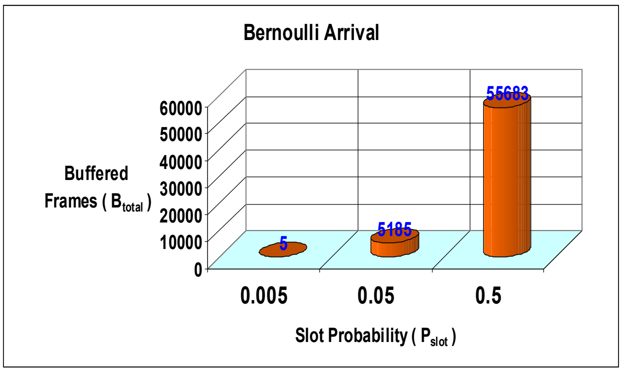

Fig. 24 Comparison between buffered frames for different P_{slot} values using Bernoulli arrival.

$$B_{total(P_{slot},Bernoulli)} = \mu P_{slot} - \rho \quad (9)$$

where $\mu \leq 112375, \rho \leq 500$

Tables XI to XIII show the effect of both P_{slot} and γ on the effectiveness of vehicular communication using F_{gen}, G_{avg}, S_{avg}, and N1, N2 as supporting data. It is clear drom the Tables, that as P_{slot} increases so do the generated frames with Bernoulli having the lowest values at P_{slot}=0.005, and Gaussian having lowest values at γ=32.

The Data also shows that using Bernoulli will result in very high frames generation at P_{slot} =0.05, and 0.5, exceeding Gaussian, while using Gaussian results in gradual decrease in the generated frames as a function of γ. This gives better control and better performance, by optimizing the spread of the Gaussian interpolation.

The presented data demonstrates that in the case of Gaussian arrival, the number of points before the inflection point and functional shape change increase as a function of both γ and P_{slot}. This indicates an increase in communication channel effectiveness and reduction in collisions.

TABLE XI
COMPARISION BETWEEN BRNOULLI AND GAUJSSIAN PARAMETERS A[41]S A FUNCTION OF SLOT PROBABILITY

P_{slot}=0.005					
γ	N_1	N_2	G_{avg}	S_{avg}	F_{gen}
2	0	15	1.199	0.488	27555
4	0	15	1.196	0.487	17979
8	1	14	1.170	0.466	10799
16	2	13	1.137	0.440	6015
32	4	11	1.066	0.402	3220
Bernoulli	15	0	0.220	0.200	585

TABLE XII
COMPARISION BETWEEN BRNOULLI AND GAUJSSIAN PARAMETERS AS A FUNCTION OF SLOT PROBABILITY

P_{slot}=0.05					
γ	N_1	N_2	G_{avg}	S_{avg}	F_{gen}
2	0	15	1.198	0.491	25834
4	0	15	1.190	0.484	16556
8	1	14	1.169	0.463	9973
16	2	13	1.138	0.436	5531
32	4	11	1.058	0.399	2946
Bernoulli	2	13	1.136	0.439	5648

TABLE XIII
COMPARISION BETWEEN BRNOULLI AND GAUJSSIAN PARAMETERS AS A FUNCTION OF SLOT PROBABILITY

P_{slot}=0.5					
γ	N_1	N_2	G_{avg}	S_{avg}	F_{gen}
2	1	14	1.166	0.464	9405
4	2	13	1.137	0.438	5486
8	4	11	1.065	0.397	3114
16	6	9	0.907	0.342	1648
32	11	4	0.468	0.275	836
Bernoulli	0	15	1.197	0.490	56171

IV. CONCLUSION

This work investigated using MATLAB simulation and found the effect of Gaussian arrival on effective throughput, data traffic, and buffered frames. It also compares the effectiveness and control of data traffic with the known Bernoulli arrival. The simulated results showed that there is a difference in the shape function between Bernoulli response (G, S) and Gaussian response (G, S, γ), with similar shapes in agreement as a function of different Pslot. The results presented effect of slot probability on G, S, and Btotal and proved that using Gaussian arrival will enable better, smoother, and more stable communication between vehicles with lower collisions and buffering. This is a function of both Pslot, and Gaussian γ. The work also shoe=wed that tuning and optimization is possible in the case of Gaussian arrival, due to its interpolation and adaptive nature. This is not possible for Bernoulli as it has a binary nature.

ACKNOWLEDGMENT

The MATLAB simulation in this work initially used and modified an algorithm originated by An-Che Teng.

REFERENCES

[1] K. Suganthi, M. A. Kumar, N. Harish, S. HariKrishnan, G. Rajesh, and S. S. Reka, "Advanced Driver Assistance System Based on IoT V2V and V2I for Vision Enabled Lane Changing with Futuristic Drivability," *Sensors*, vol. 23, no. 7, pp. 1–13, 2023, doi:10.3390/s23073423.

[2] H. Song, F. Zhao, G. Zhu, and Z. Liu, "Impacts of Connected and Autonomous Vehicles with Level 2 Automation on Traffic Efficiency and Energy Consumption," *J. Adv. Transp.*, vol. 2023, 2023, doi:10.1155/2023/6348778.

[3] C. Xu, S. Wang, P. Song, K. Li, and T. Song, "Intelligent Resource Allocation for V2V Communication with Spectrum–Energy Efficiency Maximization," *Sensors*, vol. 23, no. 15, pp. 1–16, 2023, doi: 10.3390/s23156796.

[4] A. Ahmed and B. Aijaz, "A Case Study on the Potential Applications of V2V Communication for Improving Road Safety in Pakistan," *Eng. Proc.*, vol. 32, no. 1, pp. 1–9, 2023, doi:10.3390/engproc2023032017.

[5] M. Alsudani and T. Ozturk, "Wireless Communication Between Vehicles : Exploring the Potential of V2V and V2X Communication for Improved Efficiency , Safety , and Sustainability," no. August, pp. 2–7, 2023.

[6] Y. Chen, Z. Zhan, and W. Zhang, "MPC-based time synchronization method for V2V (vehicle-to-vehicle) communication," *Railw. Sci.*, vol. 2, no. 1, pp. 101–120, 2023, doi: 10.1108/rs-01-2023-0002.

[7] A. Alsaleh, "How Do V2V and V2I Messages Affect the Performance of Driving Smart Vehicles?," *Comput. Syst. Sci. Eng.*, vol. 47, no. 2, pp. 2313–2336, 2023, doi: 10.32604/csse.2023.039682.

[8] Y. Zhang, T. Zhu, and C. Li, "Efficient Communications in V2V Networks with Two-Way," pp. 1–18, 2023.

[9] L. Peng, J. Huang, T. Zhou, and S. Xu, "V2V-enabled cooperative adaptive cruise control strategy for improving driving safety and travel efficiency of semi-automated vehicle fleet," *IET Intell. Transp. Syst.*, 2023, doi: 10.1049/itr2.12402.

[10] G. Ali, M. ElAffendi, and N. Ahmad, "BlockAuth: A blockchain-based framework for secure vehicle authentication and authorization," *PLoS One*, vol. 18, no. 9, p. e0291596, 2023, doi:10.1371/journal.pone.0291596.

[11] J. Lim, D. Pyun, D. Choi, K. Bok, and J. Yoo, "Efficient Dissemination of Safety Messages in Vehicle Ad Hoc Network Environments," *Appl. Sci.*, vol. 13, no. 11, 2023, doi: 10.3390/app13116391.

[12] M. A. Al-absi *et al.*, "Secure and efficient high throughput medium access control for vehicular ad-hoc network," *Sensors*, vol. 21, no. 14, pp. 1–24, 2021, doi: 10.3390/s21144935.

[13] R. Zhou, "VANET Architecture Analysis and Protocols," *Int. J. Comput. Appl.*, vol. 184, no. 13, pp. 44–54, 2022, doi:10.5120/ijca2022922129.

[14] N. H. Hussein, C. T. Yaw, S. P. Koh, S. K. Tiong, and K. H. Chong, "A Comprehensive Survey on Vehicular Networking: Communications, Applications, Challenges, and Upcoming Research Directions," *IEEE Access*, vol. 10, no. August, pp. 86127–86180, 2022, doi: 10.1109/ACCESS.2022.3198656.

[15] S. Y. Han and C. Y. Zhang, "ASMAC: An Adaptive Slot Access MAC Protocol in Distributed VANET," *Electron.*, vol. 11, no. 7, 2022, doi:10.3390/electronics11071145.

[16] J. Tiwari, M. Purna, A. Prakash, and R. Tripathi, "A hybrid-spatially distributed multichannel MAC protocol for vehicular ad-hoc networks," *Int. J. Electron.*, vol. 110, no. 5, pp. 955–970, 2023, doi:10.1080/00207217.2022.2068197.

[17] K. Abid, H. Lakhlef, and A. Bouabdallah, "Preventive Time Slot Allocation MAC Protocol for Vehicular Networks," *2023 Int. Wirel. Commun. Mob. Comput. IWCMC 2023*, no. June, pp. 739–744, 2023, doi: 10.1109/IWCMC58020.2023.10182516.

[18] N. N. Linn, K. Liu, and Q. Gao, "A Contention-Free Cooperative MAC Protocol for Eliminating Heterogenous Collisions in Vehicular Ad Hoc Networks," *Sensors*, vol. 23, no. 2, 2023, doi:10.3390/s23021033.

[19] L. Hota, B. P. Nayak, A. Kumar, G. G. N. Ali, P. Han, and J. Chong, "An Analysis on Contemporary MAC Layer Protocols in Vehicular Networks : State-of-the-Art and Future Directions," pp. 1–45, 2021.

[20] C. D. Ozkaptan, E. Ekici, C. H. Wang, and O. Altintas, "Neighbor Discovery and MAC Protocol for Joint Automotive Radar-Communication Systems," *IEEE Veh. Technol. Conf.*, vol. 2021-September, pp. 1–6, 2021, doi: 10.1109/VTC2021-Fall52928.2021.9625465.

[21] Z. Ming, X. Liu, X. Yang, and M. Wang, "An Improved CSMA/CA Protocol Anti-Jamming Method Based on Reinforcement Learning," *Electron.*, vol. 12, no. 17, 2023, doi: 10.3390/electronics12173547.

[22] L. Li, Y. Dong, C. Pan, and P. Fan, "Age of Information of CSMA/CA Based Wireless Networks," *2022 Int. Wirel. Commun. Mob. Comput. IWCMC 2022*, pp. 530–535, 2022, doi:10.1109/IWCMC55113.2022.9824704.

[23] A. Achroufene, M. Chelik, and N. Bouadem, "Modified CSMA/CA protocol for real-time data fusion applications based on clustered WSN," *Comput. Networks*, vol. 196, no. June, p. 108243, 2021, doi:10.1016/j.comnet.2021.108243.

[24] Z. Zheng, S. Jiang, R. Feng, L. Ge, and C. Gu, "An adaptive backoff selection scheme based on Q-learning for CSMA/CA," *Wirel. Networks*, vol. 20, no. 2018, pp. 11–13, 2023, doi: 10.1007/s11276-023-03257-0.

[25] L. K. Ouladdjedid and B. Brik, "Dynamic Beacon Distribution Mechanism for Internet of Vehicles: An Analytical Study," *Electron.*, vol. 12, no. 4, 2023, doi: 10.3390/electronics12040818.

[26] H. Ding, W. Pei, Y. Yu, P. Hu, B. Li, and X. Lu, "New Multipriority and Variable Duration Triple Time Slot P-CSMA Protocol for Edge Servers Server Deployment," *Int. J. RF Microw. Comput. Eng.*, vol. 2023, 2023, doi: 10.1155/2023/3110383.

[27] A. Baiocchi, "Maximizing the stable throughput of heterogeneous nodes under airtime fairness in a CSMA environment," *Comput. Commun.*, vol. 210, no. July, pp. 229–242, 2023, doi:10.1016/j.comcom.2023.08.010.

[28] L. Lusvarghi, A. Molina-Galan, B. Coll-Perales, J. Gozalvez, and M. L. Merani, "A comparative analysis of the semi-persistent and dynamic scheduling schemes in NR-V2X mode 2," *Veh. Commun.*, vol. 42, p. 100628, 2023, doi: 10.1016/j.vehcom.2023.100628.

[29] M. Z. Iskandarani, "Sinusoidal Regression Modelling of Vehicular Data Communication Employing NP-CSMA," *Int. J. Intell. Eng. Syst.*, vol. 16, no. 3, pp. 625–640, 2023, doi: 10.22266/ijies2023.0630.50.

[30] T. A. Alani and S. A. Aliesawi, "Driverless Cars with Communication System Based On Multiple Access Protocols," *IOP Conf. Ser. Mater.*

Sci. Eng., vol. 1076, no. 1, p. 012039, 2021, doi: 10.1088/1757-899x/1076/1/012039.

[31] Z. Han, H. Ding, K. Yue, L. Bao, and Z. Yang, "New type NP-CSMA of adaptive multi-priority control WSN protocol analysis," *Int. J. Reason. Intell. Syst.*, vol. 13, no. 1, pp. 24–31, 2021, doi:10.1504/IJRIS.2021.113049.

[32] H. S. Bedi, K. K. Sharma, S. R. A. J. Chopra, and B. Singh, "Analysis of Qos Parameters Using Different Back Off Window Algorithm in the Ieee 802 . 11E Networks," vol. 21, no. 10, pp. 6147–6157, 2022.

[33] A. M. Hamzah and Y. J. K. Nukhailawi, "The Backoff in Intermediate Networks for a Real-Time System Embedded Ethernet," *Proc. - CSCTIT 2022 5th Coll. Sci. Int. Conf. Recent Trends Inf. Technol.*, pp. 277–281, 2022, doi: 10.1109/CSCTIT56299.2022.10145655.

[34] C. Jangkajit and C. Suwannapong, "Performance Evaluation of Triangular Number Sequence Backoff Algorithm for Constrained Application Protocol," *Int. J. Technol.*, vol. 14, no. 2, pp. 399–410, 2023, doi: 10.14716/ijtech.v14i2.5686.

[35] K. Hussain, Y. Xia, and A. N. Onaizah, "Starvation mitigation and priority aware of CSMA/CA in WSN with implementing Markov chain model," *Optik (Stuttg).*, vol. 271, no. December, pp. 1–6, 2022, doi: 10.1016/j.ijleo.2022.170186.

[36] A. Baiocchi, "Age of Information in CSMA-Based Networks With Bursty Update Traffic," *IEEE Access*, vol. 10, pp. 44088–44105, 2023, doi: 10.1109/ACCESS.2022.3168321.

[37] D. Cirimelli-low, "Making CSMA Collision-Free and Stable Using Collaborative Indexing," pp. 1–8, 2022, doi: 10.1007/978-3-031-17436-0.

[38] I. S. In and I. S. In, "Throughput Estimation of slotted np-CSMA based on semi-Markov process," pp. 9–11, 2019, doi:10.1109/iEECON45304.2019.8939013.

[39] I. A. Aref, T. A. El-Mihoub, and K. A. Ben Musa, "Design Channel Nonpersistent CSMA MAC Protocol Model for Complex Wireless Systems Based on SoC Methodology," no. Ccit, pp. 182–185, 2014, doi: 10.2991/ccit-14.2014.48.

[40] P. K. Wong, D. Yin, and T. T. Lee, "Analysis of non-persistent CSMA protocols with exponential backoff scheduling," *IEEE Trans. Commun.*, vol. 59, no. 8, pp. 2206–2214, 2011, doi:10.1109/TCOMM.2011.051811.100241.

[41] C. Li, J. Yu, W. Chen, K. Wang, and K. Yang, "Measurements and analysis of vehicular radio channels in the inland lake bridge area," 2019, doi: 10.1049/iet-map.2018.5876.